**ATOMIC ENERGY
OF CANADA LIMITED**

**L'ÉNERGIE ATOMIQUE
DU CANADA LIMITÉE**

CHEMISTRY OF UO₂ FUEL DISSOLUTION

IN RELATION TO THE DISPOSAL OF USED NUCLEAR FUEL

CHIMIE DE LA DISSOLUTION DU COMBUSTIBLE D'UO₂ EN RAPPORT

AVEC LE STOCKAGE PERMANENT DU COMBUSTIBLE NUCLÉAIRE USÉ

S. Sunder, D. W. Shoesmith

AECL RESEARCH

CHEMISTRY OF UO$_2$ FUEL DISSOLUTION
IN RELATION TO THE DISPOSAL OF USED NUCLEAR FUEL

by

S. Sunder and D.W. Shoesmith

.

CHIMIE DE LA DISSOLUTION DU COMBUSTIBLE D'UO$_2$ EN RAPPORT AVEC LE STOCKAGE PERMANENT DU COMBUSTIBLE NUCLÉAIRE USÉ

par

S. Sunder et D.W. Shoesmith

RÉSUMÉ

Dans ce rapport, on examine la chimie de la dissolution de l'UO$_2$ dans des conditions se rapportant au stockage permanent du combustible nucléaire usé dans une enceinte construite en formation géologique. Il permet la connaissance chimique nécessaire pour sélectionner le modèle le plus approprié de calcul de la vitesse de dissolution du combustible d'UO$_2$ dans une enceinte de stockage permanent de déchets nucléaires. Il décrit brièvement la structure à l'état solide de divers oxydes d'uranium; il examine la nature et le mécanisme de l'oxydation et de la dissolution de l'UO$_2$ dans les eaux souterraines; il résume les facteurs influant sur la dissolution de l'UO$_2$ dans des conditions oxydantes; il examine l'impact de divers oxydants et de la radiolyse de l'eau sur l'oxydation et la dissolution de l'UO$_2$; il donne de brèves remarques sur les conséquences de la chimie de l'enceinte et de la formation de la phase secondaire pour le processus de dissolution; il examine les propriétés physiques de l'UO$_2$ qui pourraient influer sur la vitesse de dissolution; il décrit notre méthode de réalisation d'un modèle cinétique de dissolution de l'UO$_2$ dans des conditions oxydantes.

CHEMISTRY OF UO_2 FUEL DISSOLUTION
IN RELATION TO THE DISPOSAL OF USED NUCLEAR FUEL

by

S. Sunder and D.W. Shoesmith

ABSTRACT

This report reviews the chemistry of UO_2 dissolution under conditions relevant to the disposal of used nuclear fuel in a geological vault. It provides the chemical understanding necessary for selecting the most appropriate model for estimating UO_2 fuel dissolution rates in a nuclear waste disposal vault. The report briefly describes the solid-state structures of various uranium oxides; discusses the nature and mechanism of UO_2 oxidation and dissolution in groundwaters; summarizes the factors affecting UO_2 dissolution under oxidizing conditions; discusses the impact of various oxidants and water radiolysis on UO_2 oxidation and dissolution; briefly comments on the effects of vault chemistry and secondary phase formation on the dissolution process; discusses the physical properties of UO_2 that may influence the kinetics of dissolution; and describes our approach for developing a kinetic model of UO_2 dissolution under oxidizing conditions.

CONTENTS

1. INTRODUCTION

CANDU* fuel is composed mainly of UO_2, which has a very low solubility ($\sim 10^{-10}$ mol$\cdot$kg^{-1}) in water under reducing conditions [1]. In the proposed concept for disposal of used fuel in plutonic rock of the Canadian Shield, the dissolution rate of the UO_2 waste form is calculated using a solubility-limited model [2]. The dissolution rate is assumed to be directly proportional to the difference between the concentration of dissolved uranium and the equilibrium solubility of UO_2.

Although the deep granitic groundwaters found at the planned depth of a disposal vault (500 to 1000 m) are generally reducing, the redox conditions may be modified as a result of the radiolysis of groundwater by the ionizing radiation associated with the used fuel. The nature of the buffer, backfill and container materials will also influence the redox conditions of the groundwater reaching the used fuel. Therefore, it is important to understand the dissolution behaviour of UO_2 under a variety of redox and chemical conditions to select the most appropriate model for estimating UO_2 dissolution rates, and hence radionuclide release rates, in the vault. Under oxidizing conditions, the dissolution rate of UO_2 will not be controlled by the solubility of a single uranium phase. Since oxidative dissolution will be an irreversible process, one must take into account the kinetics of steps involved in UO_2 oxidation and dissolution [3].

In this review we will confine ourselves to a discussion of the oxidative dissolution of UO_2, very little work having been done on dissolution under reducing conditions. The fate of dissolved uranium in the near-field environment of the vault will not be considered. Hence, the results will define the conditions for the release of radionuclides from the fuel but not from the vault. The impact of near-field chemistry will be considered only in so far as it exerts a direct impact on the mechanism and/or kinetics of fuel dissolution. This review includes the following:

(i)   a brief description of the structural properties of uranium
      oxides;

(ii) a discussion of the nature and mechanism of UO_2 dissolution;

(iii) a summary of the factors affecting UO_2 dissolution under oxidiz-
      ing conditions;

(iv) a review of the impact of various oxidants that could drive the
      oxidative dissolution of UO_2, including the impact of water
      radiolysis products;

(v)   a few comments on the impact of vault chemistry and secondary
      phase formation on the dissolution process;

(vi) a discussion of the physical factors likely to influence the
      kinetics of dissolution; and

(vii) a brief description of our approach to modelling of UO_2
      dissolution.

A more extensive review of some of these topics has been published earlier
by Johnson and Shoesmith [4].

2.   STRUCTURAL AND SOLID-STATE PROPERTIES OF URANIUM OXIDES

The dissolution of UO_2 will occur from a surface of UO_{2+x}, where x is
determined by the redox conditions established at the dissolving surface.
The surface composition and the properties of the surface layers, such as
semiconducting properties, are expected to influence not only the kinetics
of the anodic dissolution process but also the kinetics of the cathodic
reaction during the dissolution, and may, therefore, exert a significant
impact on the overall dissolution rate.

The chemistry of uranium oxides is complex, and has been frequently reviewed. A review by Smith et al. summarizes recent literature for the phase relations and crystal structures in the uranium-oxygen-water system and their significance to the stability of nuclear waste forms [5]. In this section, we will briefly review the phase relationships, crystal structures and semiconducting properties of those phases that might have an impact on UO_2 reactivity (specifically oxidative dissolution), and hence on radionuclide release. As we will see in the later sections, many of these phases are formed during the oxidative dissolution of UO_2.

In the UO_2-U_4O_9 range, all the known phases are based on the fluorite structure. As the composition deviates from $UO_{2.00}$ (to UO_{2+x}), the unit-cell size shrinks and it has been shown, by density and X-ray measurements, that UO_{2+x} is an oxygen-excess structure, with the extra oxygen atoms occupying interstitial positions in the UO_2 lattice [6]. Neutron diffraction measurements have shown that a number of specific defect structures are formed without major disruption of overall lattice symmetry [7-9].

Conductivity measurements have shown that the introduction of oxygen at interstitial sites leads to an approximate hundredfold increase in electrical conductivity between the composition $UO_{2.00}$ and $UO_{2.06}$ [10-12]. The conductivity is p-type, owing to the transport of positive holes formed by uptake of the interstitial oxygens. Conduction is thought to occur via a hopping mechanism as the holes jump between uranium cation sites [11]. The semiconductor band gap is ~2.0 eV [10], the electronic transition being an intracationic f-d transition [13-14] from the 5f valence states that are localized in UO_2.

The composition $UO_{2.25}$ shows evidence of ordered structures based on the fluorite structure, with the uranium atoms undergoing small systematic displacements [9], which allow accommodation of interstitial oxygen and result in observable superstructures. These phases are generally designated U_4O_9, but, depending on heat treatment and redox conditions, are often non-stoichiometric and occur together with UO_{2+x} [10]. Non-stoichiometric U_4O_9 generally exhibits n-type conduction [11,15] and has been described as anion-deficient [10]. Hence, as the O/U ratio increases from ~2.00 to

~2.25, mixed p-type/n-type conductivity becomes possible. Since n-type sites might be expected to support cathodic processes while p-type sites support anodic dissolution, mixed conduction could lead to heterogeneous dissolution.

Several different phases, compositionally near $UO_{2.3}$, have been reported. These "U_3O_7" phases are obtained by oxidation of UO_2 and U_4O_9. The phase α-U_3O_7 is tetragonal with a distorted fluorite structure; hence it can be considered an extension of the UO_{2+x} and U_4O_{9-y} structures [16]. Although designated U_3O_7, the composition is more likely close to $UO_{2.27}$ and appears to be an anion-deficient semiconductor with n-type conductivity [10,15].

The U_3O_7 phase is effectively the end of the fluorite-structure range. The composition U_2O_5 has been reported, but is thought to exist only at high pressures ($>10^3$ MPa) [17]. The three distinct phases with this U_2O_5 composition (α, β, γ) appear to have structures intermediate between the UO_2-like (fluorite) structure and the layer structure encountered in the orthorhombic higher oxides. This composition has been claimed to represent the change from U^{4+} and U^{5+}, which appear to control the structures of the lower oxides, to U^{5+} and U^{6+}, which control the structures of the higher oxides [5]. As is discussed later, it is around this composition that oxide dissolution, as U^{6+}, starts to dominate the redox chemistry.

In the composition range from U_2O_5 to U_3O_8, up to twelve distinct phases have been reported, though α-U_3O_8 is generally the phase formed by UO_2 oxidation or by thermal decomposition of uranyl salts [5]. In α-U_3O_8, all of the uranium atoms are seven-coordinate; UO_7 pentagonal dipyramids share equatorial edges and corners to form infinite sheets, which are linked through axial oxygens to adjacent sheets [18]. The two axial oxygens are at shorter distances than the equatorial oxygens and can be related to the "uranyl moiety" in these solids. This structure does not differ significantly for all compositions in the range from U_2O_5 to UO_3. Generally, U_3O_8 is non-stoichiometric, U_3O_{8-F}; the oxygen deficiency yielding n-type semiconducting properties [10,15,19].

Uranium normally does not form hydrated oxides until it is fully oxidized to U^{6+}, with $UO_3 \cdot 2H_2O$ being the stable hydrate around room temperature [20]. The phase $UO_2(OH)_2$ is of interest in dissolution kinetics, since it appears to limit oxidative dissolution rates in alkaline solutions. This compound possesses a layered structure of uranyl groups bonded to hydroxyl groups, and it is an expected oxidation product of U_3O_8 in aqueous solutions. Alternatively, the electrochemical oxidation of U_3O_8 could produce the anhydrous $\alpha\text{-}UO_3$, which is close in structure to U_3O_8. The uranium trioxide-water system has been discussed in detail by several authors, e.g., Hoekstra and Siegel [21], Smith et al. [5], and O'Hare et al. [20]. A comprehensive review of literature until 1978 on the U_3O_8 and UO_3 structures is given by Keim [22].

3. NATURE AND MECHANISM OF UO_2 DISSOLUTION

Bruno et al. [23] have claimed that the rate of dissolution under nominally reducing conditions, achieved by bubbling H_2 gas through solutions in the presence of a Pd catalyst, is related to the solubility of UO_2. The rate was found to decrease with increasing acidity, suggesting a hydroxo-promoted dissolution reaction via the formation of a surface complex with OH^- ions.

Reducing conditions are difficult to achieve and the majority of studies of UO_2 dissolution have involved the presence of at least minor amounts of oxidants. The oxidative dissolution of UO_2 has been demonstrated to be an electrochemical reaction in the presence of various oxidizing agents by Nicol, Needes and Finkelstein [24,25]. This means that the reaction can be envisaged as composed of an anodic dissolution half reaction ($UO_2 \rightarrow UO_2^{2+}$ + 2e) driven by a cathodic reduction half reaction (Ox + 2e $\rightarrow$ Red). Such half reactions are most conveniently studied by electrochemical techniques, the electrochemical current being a direct measure of their rate. Hence, one can estimate dissolution rates under various oxidizing conditions by using standard polarization techniques, i.e., by measuring steady-state currents under electrochemically controlled potentials and extrapolating

them to the observed corrosion potentials [26]. As illustrated in Figure 1, one plots the observed steady-state currents on a UO_2 electrode as a function of applied potential and extrapolates these curves to the measured value of the corrosion potential to determine the dissolution currents (rates) under natural corrosion conditions. The corrosion current is, of course, specific to the conditions under which the measurement is made.

We have used electrochemical methods, complemented by surface-spectroscopic techniques (particularly X-ray photoelectron spectroscopy, XPS), to study the oxidation and dissolution of UO_2 [27-45]. The methodology used in these studies has been described elsewhere [37]. These studies provide not only information on the mechanism of dissolution of UO_2 under different chemical conditions, but also criteria for determining conditions under which one can either (i) apply a solubility-limited model or (ii) use a kinetic corrosion model to estimate used-fuel dissolution rates. If a kinetic model is used, these studies will provide the values for the parameters upon which such a model will be based.

Oxidative dissolution of UO_2 can be represented in terms of five stages, as shown schematically in Figure 2. Stage 1 in this figure represents the primary step of UO_2 oxidation and the formation of an oxidized film on the fuel surface. Stage 2 represents the formation of the UO_2^{2+} ion on the oxidized film and its subsequent dissolution. These two stages (1 and 2) are determined by the surface redox conditions, i.e., the balance of kinetics between the anodic reaction (oxidation of UO_2) and the cathodic reaction (reduction of the oxidizing agent). The corrosion rate will also be influenced by the reactivity of the fuel sample, which in turn will be determined by the physical and chemical properties of both the uranium oxide matrix and its surface. The redox conditions are established by the radiolysis of groundwater and the redox couples present in it, as indicated in the top section of the figure. The complexation of uranyl ion in the groundwater, represented by stage 3 in Figure 2, is determined by the groundwater composition. Complexation can have a direct influence on dissolution (stage 2), as well as affecting stages 4 and 5. Stage 4 represents the precipitation of secondary phases. It may affect dissolution,
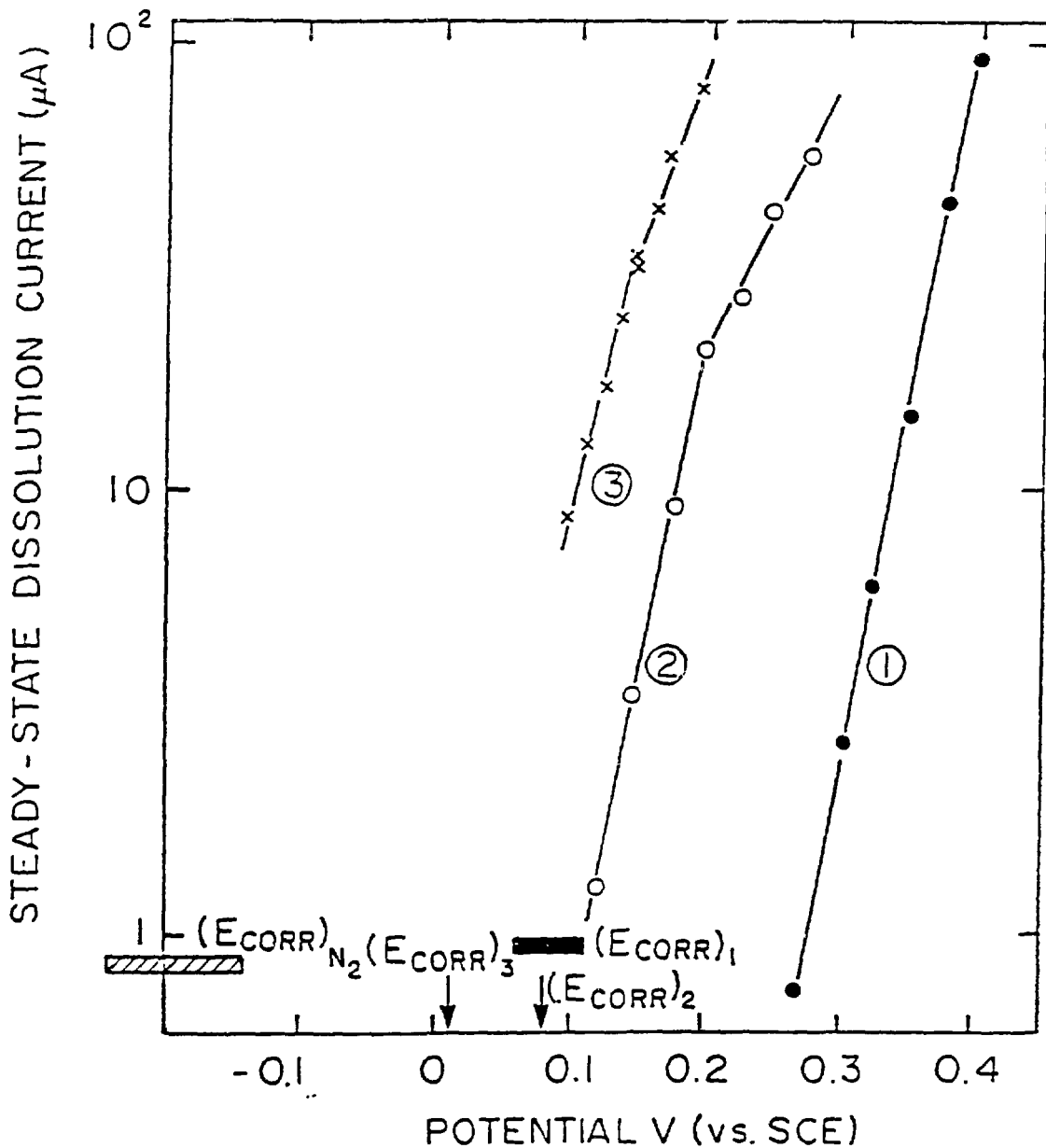
FIGURE 1: Plots of Steady-State Dissolution Current as a Function of
Applied Potential in (1) 0.1 mol·dm^{-3} NaClO$_4$ (pH = 9.5);
(2) 0.1 mol·dm^{-3} NaClO$_4$ + 0.01 mol·dm^{-3} NaHCO$_3$ (pH = 9.5);
(3) 0.1 mol·dm^{-3} NaClO$_4$ + 0.5 mol·dm^{-3} NaHCO$_3$ (pH = 9.3).   The
solid horizontal bar and vertical arrows represent the range of
values or single values recorded for UO$_2$ corrosion potential in
the corresponding O$_2$-saturated solutions. (E$_{CORR}$)$_{N2}$ shows the
range of E$_{CORR}$ values observed in N$_2$-purged 0.1 mol·dm^{-3} NaClO$_4$
(pH = 9.5) solutions.

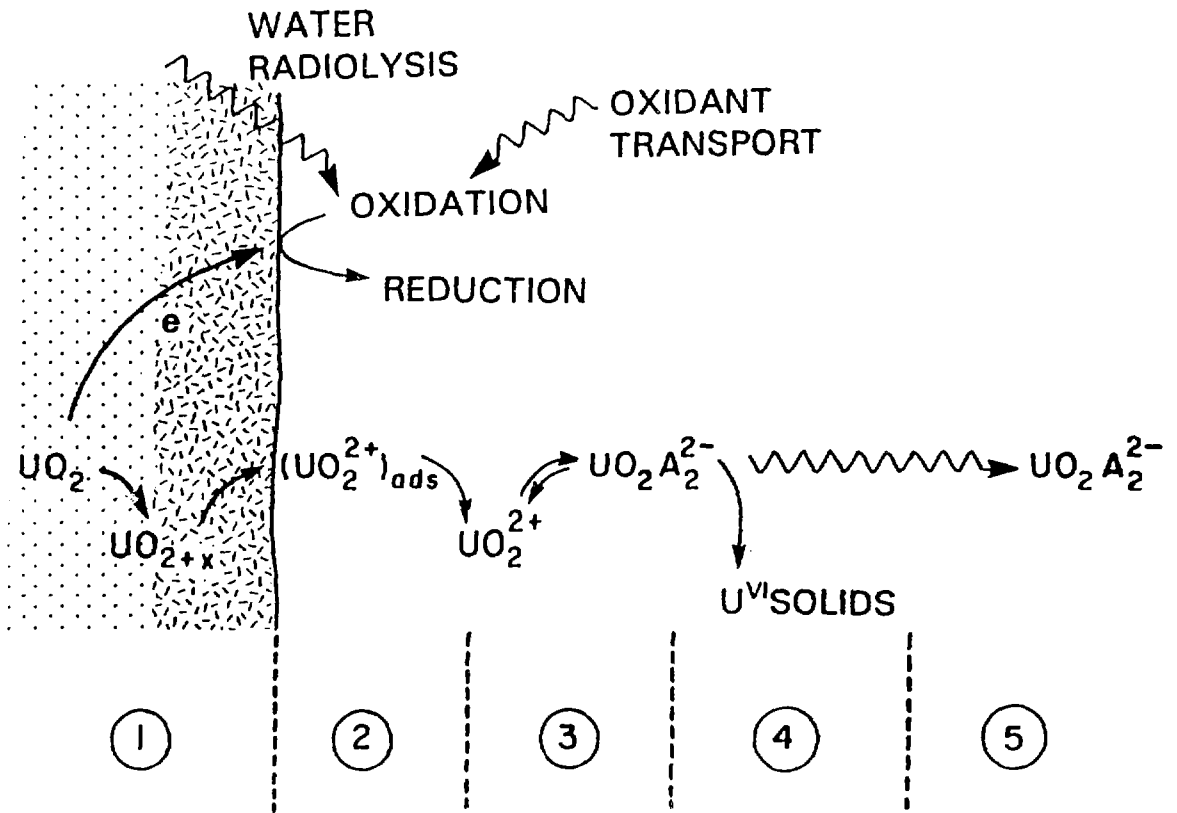FIGURE 2: Schematic Representation of Processes Occurring During Oxidative Dissolution of UO_2 in a Geological Vault

depending upon the relative location of the precipitation site and the fuel surface. Stage 5 represents the transport of uranium species and will be influenced by groundwater composition, the presence of colloids, and the density and composition of the compacted clay/sand mixture packed around the waste package.

4. ELECTROCHEMISTRY OF UO_2 DISSOLUTION

The mechanism of dissolution of UO_2 has been studied in detail as a function of many parameters, including redox potential, concentration of species in groundwater and temperature. The impact of these parameters is summarized below.

4.1   REDOX POTENTIAL

Redox potential is the most important parameter governing the dissolution of UO_2 and the release of radionuclides. In the absence of strongly complexing anions, the mechanism of oxidation and dissolution of UO_2 in neutral and basic solutions can be described by the set of reactions shown in Figure 3 [29]. Surface oxidation of UO_2 can occur at very low, quite negative potentials (-800 to -400 mV), but is confined to a few monolayers or to specific areas of the surface, Reaction (a) in Figure 3. At more oxidizing potentials, a layer of $UO_{2.33}$ is formed via Reactions (b) and (c). These early stages of oxidation appear to involve the incorporation of oxygen at interstitial sites in the fluorite lattice of UO_2, and no drastic change in lattice structure is required until a limiting stoichiometry of $\sim UO_{2.33}$ (U_3O_7) is reached. This phase is effectively the end of the fluorite structural range, as discussed in Section 2. The solid-state conversion of $UO_{2.33}$ to higher oxides, Reactions (d), (e) and (f), is observed at room temperature under electrochemical conditions. Oxidation beyond the $UO_{2.33}$ stage involves a major change in the crystallographic lattice and is accompanied by extensive dissolution, Reactions (g), (h) and (j). Significant oxidative dissolution appears possible for potentials more positive than -100 mV (vs. SCE).

The electrochemical formation of phases such as U_2O_5 and U_3O_8 only occurs at very positive potentials [27]. These potentials are much more positive than those achievable for corrosion in aerated solutions [41]. Consequently, oxidative dissolution under natural corrosion conditions is expected to proceed via steps (g), (h) and (j), not (d), (e) and (f).

4.2 GROUNDWATER COMPOSITION

4.2.1 pH

The pH of the groundwater has a pronounced effect on the oxidative dissolu-
tion of UO_2. It affects both the nature of the films formed on UO_2 and
their rate of dissolution. For pH < 5, dissolution proceeds with little
surface oxidation; i.e., Reactions (g) and (h) are strongly favoured over
Reactions (d), (e) and (f) in Figure 3. Below a pH of 5, surface films of
composition $UO_{2+x}/UO_{2.33}$ do not appear to restrict oxidative dissolution.
The thickness of this oxidized surface film ($UO_{2+x}/UO_{2.33}$) increases with
pH, particularly at pH > 10. The dissolution rate appears to decrease with
an increase in pH above 5. The dissolution rate data for UO_2 under oxidiz-
ing conditions show the lowest dissolution rates for pH values between 5
and 10 [46]. It is noted here that most groundwaters have pH values rang-
ing between 6 and 9, i.e., neutral to slightly basic [47].
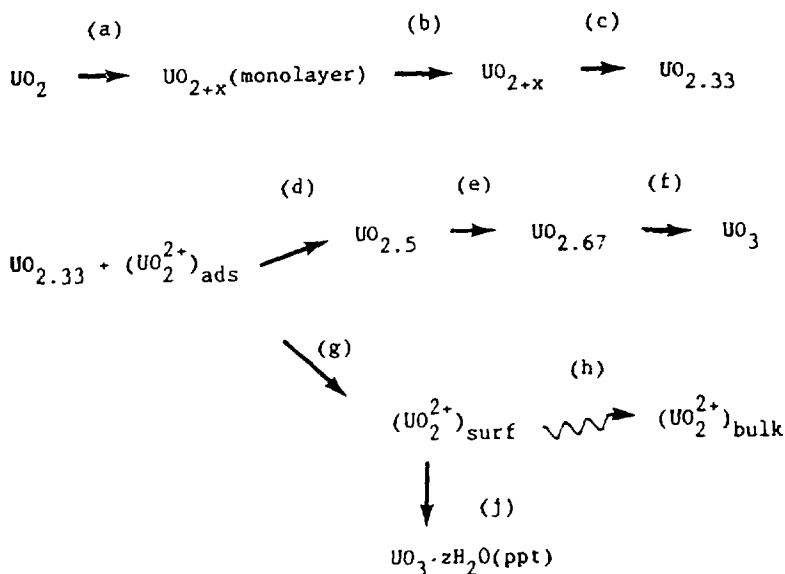
FIGURE 3: Mechanism of Oxidation and Dissolution of UO_2 as a Function of
Increasing Potential. Here, $0 < x < 0.33$, z can have various
values up to 2, $(UO_2^{2+})_{ads}$ denotes uranyl ions in solid surface,
$(UO_2^{2+})_{surf}$ denotes uranyl ions in solution close to solid
surface, and $(UO_2^{2+})_{bulk}$ denotes uranyl ions (as free UO_2^{2+}, UO_2^{2+}
complexed with anions and/or other uranyl ions, or hydrated) in
the bulk of the solution.

4.2.2   Ion Content

Both the nature and the concentration of anions present in groundwater
affect the oxidative dissolution rate. Complexing anions are expected to
accelerate dissolution by stabilizing the dissolved uranyl ions. Since
groundwater analyses show that the important anions to consider are
CO_3^{2-}/HCO_3^{-}, SO_4^{2-}, Cl^-, F^- and $H_2PO_4^-$ [47-49], we have studied the effects of
these anions in some detail (D.W. Shoesmith, unpublished data)
[29,32,33,37,39].

Anodic oxidation of UO_2 in solutions with carbonate concentrations
≥ 0.001 mol·dm^{-3} did not result in any surface film with a U(VI)/U(IV) ratio
>0.5, i.e., uranium oxides with an oxidation state higher than $UO_{2.33}$ (U_3O_7)
were not formed even at potentials much higher than the corrosion potential
[33]. In terms of the reaction scheme, Figure 3, the dissolution Reactions
(g) and (h) are obviously favoured over film formation processes (d), (e)
and (f).

Acceleration of dissolution in carbonate solutions can be attributed partly
to a thermodynamic effect and partly to a kinetic effect. The thermodynamic
effect is due to the stabilization of the dissolution product, the uranyl
ion, via the complexation equilibria:

$$UO_2^{2+} + CO_3^{2-} \rightleftharpoons UO_2CO_3(aq) \qquad \log K_1 = 9.5 \pm 0.4, \qquad (1)$$

$$UO_2^{2+} + 2CO_3^{2-} \rightleftharpoons UO_2(CO_3)_2^{2-} \qquad \log \beta_2 = 16.6 \pm 0.3, \qquad (2)$$

$$UO_2^{2+} + 3CO_3^{2-} \rightleftharpoons UO_2(CO_3)_3^{4-} \qquad \log \beta_3 = 21.3 \pm 0.6 . \qquad (3)$$

The values for the equilibrium constants for Reactions 1 to 3 are from
Reference 50, for Reactions 4, 7 and 8 are from Reference 51 and for
Reactions 5 and 6 are from Reference 49 (see below). These values are the
latest accepted values for the aqueous solution at zero ionic strength and
at 25°C. Values of these equilibrium constants for solutions at higher
ionic strength, e.g., groundwaters expected in the Canadian Shield, are
discussed in References 48 and 49. The effects of higher temperatures on
these equilibria are discussed in References 51 and 52.

Complexation favours dissolution by shifting the equilibrium potential for the anodic dissolution half reaction to more negative potentials. Also, the formation of surface complexes, such as UO_2HCO_3 and UO_2CO_3, has been shown by ac impedance experiments to accelerate the rate of anodic dissolution (D.W. Shoesmith, unpublished data) [37]. The importance of such intermediates in determining the kinetics of anodic dissolution decreases for less positive potentials and under natural corrosion conditions (i.e., at the corrosion potential) the thermodynamic influence predominates.
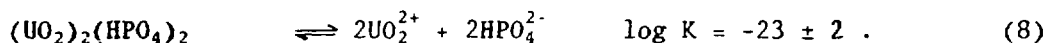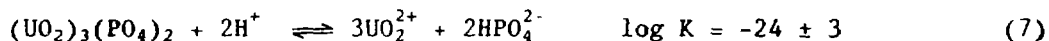
The relative effects of CO_3^{2-}, SO_4^{2-} and PO_4^{3-} ions are shown in Figure 4. The impact of SO_4^{2-} ions on the dissolution of UO_2 is minor compared with that of CO_3^{2-}. This is consistent with the lower stability of UO_2^{2+} complexes with sulphate (Reaction (4)) compared with those with carbonates (Reactions (1) to(3)):

$$UO_2^{2+} + SO_4^{2-} \rightleftharpoons UO_2SO_4(aq) \qquad \log K = 2.9 \pm 0.5 . \qquad (4)$$

The effect of phosphate ions on UO_2 dissolution is complex. Under moderately oxidizing conditions, the presence of phosphate increases the dissolution rate by its complexation with uranyl ions:

$$UO_2^{2+} + HPO_4^{2-} \rightleftharpoons UO_2HPO_4(aq) \qquad \log K_1 = 8 \pm 2 \qquad (5)$$

$$UO_2^{2+} + 2HPO_4^{2-} \rightleftharpoons UO_2(HPO_4)_2^{2-} \qquad \log \beta_2 = 17.5 \pm 2 . \qquad (6)$$

Under strongly oxidizing conditions, the presence of PO_4^{3-} limits the dissolution rate [18] by the formation of an insoluble surface layer of uranyl phosphate:

$$(UO_2)_3(PO_4)_2 + 2H^+ \rightleftharpoons 3UO_2^{2+} + 2HPO_4^{2-} \qquad \log K = -24 \pm 3 \qquad (7)$$

$$(UO_2)_2(HPO_4)_2 \rightleftharpoons 2UO_2^{2+} + 2HPO_4^{2-} \qquad \log K = -23 \pm 2 . \qquad (8)$$
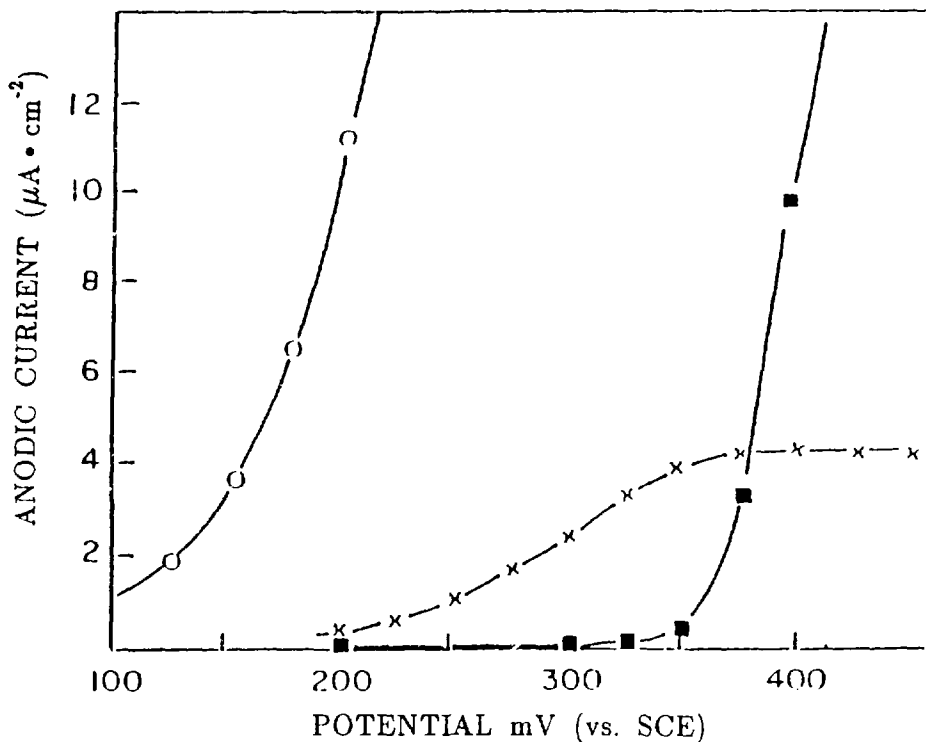
FIGURE 4: Plots of Steady-State Dissolution Current vs. Applied Potential in Solutions Containing Na_2SO_4 (pH = 9.4) (■) and in the Same Solution Containing 0.1 mol·dm^{-3} $NaHCO_3$ (O) or 0.1 mol·dm^{-3} Na_2HPO_4 (X)

The ac impedance results indicate that the phosphate ions are also directly involved in the formation of an adsorbed intermediate, though a clear mechanism has not been elucidated (D.W. Shoesmith, unpublished data). Chloride showed no significant effect for [Cl$^-$] up to 0.1 mol·dm^{-3}. Fluoride affects UO_2 dissolution only under acidic conditions, an increase in rate being observed for pH $\leq$ 4. Our electrochemical studies on the effects of anions on UO_2 dissolution are consistent with the thermodynamic calculations of Langmuir [53], and Paquette and Lemire [52].

Under less oxidizing conditions, i.e., at potentials more negative than -100 mV (vs. SCE), the dissolution of UO_2 is less sensitive to the nature and concentration of anions; i.e., oxidation must occur before complexation of the uranyl ion can accelerate dissolution. Therefore, the oxidation step dominates kinetically as the potential is made more reducing.

The nature of cations present in the groundwater does not directly affect the dissolution rate of UO_2, but could affect the nature of secondary phases formed subsequent to oxidative dissolution [54] as discussed in more detail in Section 6.

4.2.3   Colloid and Organic Content

The presence of colloids in the groundwater reaching the UO_2 fuel is not expected to affect its dissolution rate directly. The nature of colloids in the groundwater will influence the nature of the secondary phases formed after dissolution and the transport of dissolved uranium species through the vault (stages 4 and 5, Figure 2). However, very little information is available about the effects of colloids on UO_2 dissolution. Colloids containing organic material, e.g., humic acids, and/or other redox couples may influence the dissolution rate by affecting the redox potential of the groundwater.

Organic matter present in the soil and groundwaters is mainly composed of humic compounds that are organic polyelectrolytes. The presence of organic material can influence the dissolution rate by altering the mobility of the uranium moieties, i.e., by complexation, and/or by affecting the redox potential of the groundwater. The concentration of dissolved organic carbon (DOC) at the expected depth of the disposal vault is expected to be quite small. Samples from fairly deep groundwater in crystalline rock in Sweden gave DOC values ranging from 1 to 8 $mg \cdot dm^{-3}$ [55]. The complexing constants of the humic compounds with uranyl ions are expected to have values in the range log $\beta_1 = 5$ to 6.7 [56-57]. The complexing capacity of these humic compounds will be further reduced by the radiolysis of water from the loss of carboxylic groups, the main complexing sites in these compounds, by reaction with radicals formed during radiolysis [58]. Also, the mobility of humates in the compacted clay, used as a backfill around the fuel containers in the disposal vault, is expected to be very low. For example, studies of the diffusion of large organic molecules through highly compacted clays indicate that diffusion coefficients can be several orders of magnitude lower than those of uranium and mono- and divalent cations [59]. As a result, even if some complexation were to occur, the rate of

supply of humates to the fuel, as well as the rate of migration of complexed uranium (or other radionuclides) away from the fuel, would be severely limited by the slow diffusion of these species in buffer material.

The presence of organic material may also influence the dissolution rate by affecting the redox potential of the groundwater. Control of dissolution processes by organic redox couples present in groundwater has been shown to affect the dissolution of other metal oxides [60]. However, little, if anything, is known about this reactivity with uranium oxides. Also, the presence of organic matter in the groundwater may affect the oxidation of UO_2 because of the radiolysis of water (Section 5). For example, it has been shown that the presence of organics decreases the oxidation of Fe^{2+} in deaerated solutions but increases it in aerated solutions [61]. In both cases, the effect seems to result from the reaction of OH radicals with the organic molecules:

$$OH + RH = H_2O + R . \tag{9}$$

In the absence of oxygen, the organic radical, R, generally reduces ferric iron rather than oxidizing ferrous iron, with the result that an oxidizing radical, OH, is converted to a reducing one. On the other hand, in the presence of oxygen, the radical will add to oxygen to form RO_2. The RO_2 radical may either hydrolyze to HO_2 or react with ferrous ions to form a ferric ion and hydrogen peroxide, which in turn can oxidize two more ferrous ions [61]. Either way, an OH radical that can oxidize only one ferrous ion is converted into a radical, in the presence of organics, that can bring about the oxidation of three ferrous ions. Hence, the effects of organics on the redox characteristics of a solution undergoing radiolysis will depend upon the composition, in particular, the oxygen content of the solution. As the groundwater at the planned depth of the disposal vault is expected to be quite reducing [47], we believe that the presence of organics in the groundwater may reduce the possible oxidation of UO_2 as a result of the water radiolysis. Hence, we conclude that the effect of organic matter present in the groundwater reaching the used fuel in a granitic disposal vault on the kinetics of oxidative dissolution of UO_2 will be minor.

4.3   TEMPERATURE EFFECT

The temperature in the disposal vault is expected to be ~75 to ~100°C for a
considerable period (10^2 to 10^3 a), because of the energy released in the
decay of radionuclides in the used fuel. Many authors have measured acti-
vation energies for the oxidative dissolution of UO_2. These measurements
have generally been made in acidic solutions containing oxidants, such as
Fe(III) or V(V) or H_2O_2, or in carbonate solutions containing oxygen. In
acidic solutions, activation energy values range from ~50 to ~67 $kJ \cdot mol^{-1}$
[24,62-65], compared with ~43 to ~63 $kJ \cdot mol^{-1}$ in oxygenated carbonate
solutions [66-70]. In acidic solutions containing H_2O_2, a value of
~27 $kJ \cdot mol^{-1}$ was obtained [71].

All these values are consistent with a rate-determining step involving
either electron transfer or ion transfer. This is not surprising in acidic
solutions, where dissolution is uninhibited by the presence of oxidizing
surface layers. The lower activation energy measured in peroxide solutions
has been attributed to fast dissolution controlled by the mass transport of
peroxide to the UO_2 surface. In carbonate solutions, however, the presence
of $UO_{2.33}$ might be expected to decrease the dependence of dissolution rate
on temperature. That this is not the case suggests that the inhibiting
effect of such layers is minor at high carbonate concentrations
($>10^{-1}$ $mol \cdot L^{-1}$). Our own electrochemical experiments confirm that the
surface layer present under oxidizing conditions is very thin at these
concentrations [32].

Groundwaters will not achieve such acidities (pH $\leq$ 1) or carbonate contents
($>10^{-1}$ $mol \cdot L^{-1}$) and the inhibiting impact of surface layers is likely to be
more important, leading to a lower dependence of rate on temperature.
Consequently, it is unlikely that the activation energies noted above will
apply under the neutral, less complexing environment within a waste vault.
The results of Thomas and Till [46] appear to confirm this. Assuming
Arrhenius behaviour between 30 and 90°C, they calculated an activation
energy of only 20 $kJ \cdot mol^{-1}$ for dissolution in distilled water. In granitic
groundwater, the dissolution rate actually decreased with temperature,
suggesting that dissolution was inhibited by the formation of secondary
phases or mineralized layers.

The actual activation energy value calculated by Thomas and Till is undoubtedly suspect, since the nature of the dissolution process changes with temperature. A similar low dependence of oxidative dissolution rate on temperature has been observed in used-fuel dissolution studies. For measurements carried out over the temperature range 25-150°C, Johnson and Joling [72] suggested that rates increased by a factor of only 10 to 20, and a similar low dependence has been suggested by Gray and McVay [73].

Our own studies on the anodic oxidation of UO_2 at 55°C (0.1 mol·L^{-1} NaClO$_4$, pH ~ 9) show that the increase in temperature (from 25°C) does not alter the threshold potential (~-100 mV vs. SCE) for oxidative dissolution (S. Sunder and D.W. Shoesmith, unpublished data). The expected increase in the dissolution rate with temperature, due to the normally high activation energies for such processes, is offset by a thickening of the surface $UO_{2.33}$ layer. This thickening impedes transport of oxygen to the $UO_2/UO_{2.33}$ interface, where oxidation occurs. We believe that the higher than ambient temperatures expected in the disposal vault will not lead to any significant increase in the dissolution rate. In fact, higher temperatures may reduce the fuel dissolution rate by helping the formation of "protective" secondary phases (Section 6) and by increasing the activity of reductants (H_2) formed during radiolysis (Section 5.2).

5. EFFECT OF RADIOLYSIS OF WATER ON UO_2 FUEL OXIDATION AND DISSOLUTION

The main source of oxidants to drive the oxidative dissolution of UO_2 will likely be the radiolysis of water, which produces a mixture of both oxidants and reductants, including OH, O_2, O_2^-, H_2O_2, H, H_2, and e_{aq} [61]. The overall effect is expected to be oxidizing because reducing radiolysis products are kinetically inert at temperatures below ~100°C. Reducing effects may be more important at higher temperatures. The effects of the various radiolysis products on UO_2 oxidation and dissolution will be complex because of possible reactions between them, as illustrated in Figure 5. To understand their role in UO_2 oxidation and dissolution, we
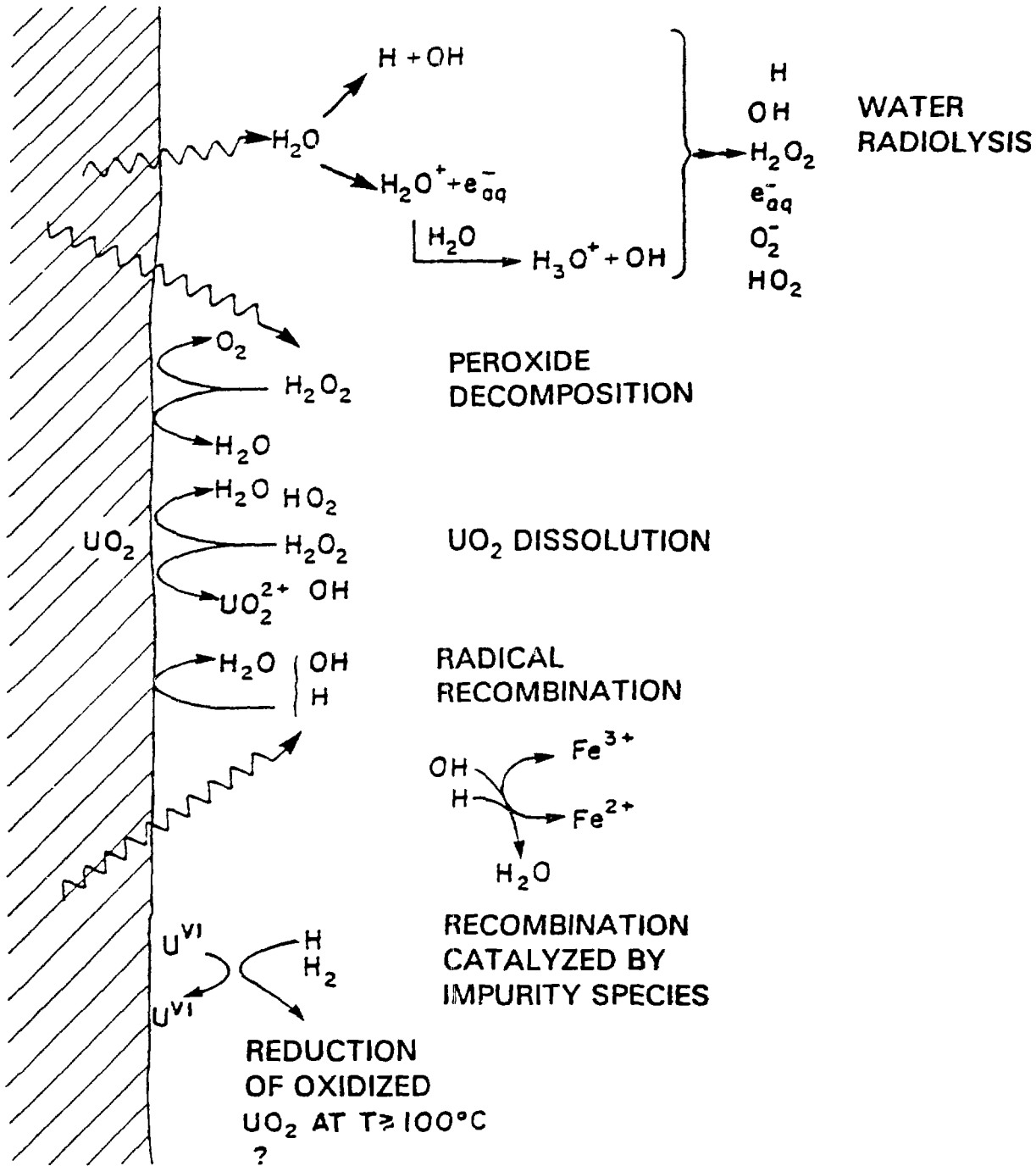
FIGURE 5: Schematic Representation of Oxidants and Reductants Formed
During Radiolysis and Their Interrelationships

have studied the effects of specific radiolysis products, in addition to the direct effects of the alpha and gamma radiolysis of water.

5.1 EFFECT OF SPECIFIC RADIOLYSIS PRODUCTS

5.1.1 Dissolved Oxygen

The effect of dissolved O_2 on UO_2 oxidation and dissolution has been studied in detail [35,38,41,45]. In solutions containing very low concentrations, i.e., less than 0.3×10^{-8} mol·dm^{-3}, of O_2, we observe no oxidative dissolution of UO_2 [38,41]. However, in neutral or alkaline aerated solutions (pH > 5), dissolution of UO_2 proceeds by the formation of two films [41]. Initially, a film of $UO_{2+x}/UO_{2.33}$ is formed whose thickness increases with pH. Outer layers of this film are slowly converted to hydrated UO_3 or a uranyl (UO_2^{2+}) complex, depending upon the nature and concentration of the complexing anions. The dissolution rate in O_2-saturated solutions increases with decreasing pH and in the presence of strongly complexing anions like CO_3^{2-} [41,45]. In acidic solutions formation of $UO_{2.33}$ film is not observed and oxidation proceeds directly to the U(VI) state. The corrosion potential suggests that anodic dissolution, rather than oxidant reduction, is rate-determining for pH > 10. For lower pH values, the corrosion potential shows only a slight dependence on pH, and the nature of the rate-determining reaction is unknown.

A knowledge of the rate-determining step in the dissolution process is impossible without a good understanding of the mechanism and kinetics of the oxidant reduction reaction. A thorough electrochemical investigation of the cathodic reduction of oxygen on UO_2 is under way using rotating ring-disk electrodes [74]. The kinetics are determined by the oxygen concentration, the extent of pre-oxidation of the electrode, the concentration of surface-adsorbing ions, such as carbonate, and other physical properties of the electrode, such as semiconducting properties.

For p-type UO_2 (the expected conduction type for UO_2, but not necessarily for used CANDU fuel), oxygen reduction is a first-order reaction in oxygen concentration, independent of pH for 8 < pH < 12, and no intermediate H_2O_2

is obtained, confirming that the overall reduction process involves four
electrons. On poorly characterized n-type UO_2, the mechanism appears to be
quite different.

5.1.2   Hydrogen Peroxide

We have studied the oxidation of UO_2 in H_2O_2 solutions as a function of its
concentration, oxidation time, solution pH and CO_3^{2-} content. We find that
the rate of UO_2 oxidation in near-neutral solutions containing hydrogen
peroxide is about 200 times faster than in the presence of dissolved oxygen
at equivalent concentrations [35]. The faster rate of oxidation in
solutions containing hydrogen peroxide is probably due to the reactions
involving radicals (vide infra), such as OH and HO_2^-, produced by the
decomposition of H_2O_2.

We have studied in detail the effect of H_2O_2 concentration on UO_2 oxidation
at pH ~ 9. The mechanism of oxidation appears to change if the concentra-
tion of H_2O_2 increases above 0.01 $mol \cdot dm^{-3}$ [38]. The predominant reactions
at lower concentrations appear to involve H_2O_2 decomposition at the UO_2
surface, while at higher concentrations the oxidative dissolution of UO_2
becomes more important.

We have also studied the effect of pH on UO_2 oxidation by H_2O_2. The
corrosion potential measurements show a shift to more positive values,
indicative of increasingly oxidizing conditions, with a decrease in pH in
the range 2-12 [38]. Our XPS studies indicate that the degree of surface
oxidation increases with a decrease in pH for pH < 6, and for pH > 10.5
(S. Sunder and D.W. Shoesmith, unpublished data). For intermediate values
of pH, the degree of surface oxidation does not change. The presence of
CO_3^{2-} anions increases the oxidative dissolution rate of UO_2 by H_2O_2
(S. Sunder and D.W. Shoesmith, unpublished data), in agreement with the
reaction scheme shown in Figure 3.

5.1.3   Radicals

The primary products of water radiolysis are radicals. We have studied the
effects of three radicals, OH, O_2^-, and CO_3^-, on the oxidation and disso-
lution of UO_2 [42,43]. Experiments were also carried out to compare the
effects of radicals and molecular oxidants. Our studies show that,
although the concentrations of the radicals in solutions undergoing radio-
lysis are very low ($<<10^{-9}$ mol·dm^{-3}), they cause oxidation of UO_2 over and
above that observed for the molecular oxidants, e.g., for H_2O_2 at concen-
trations up to 10^{-3} mol·dm^{-3} and for aerated solutions. The fastest
increase in corrosion potential, and the highest final steady-state values,
were observed in solutions favoring the formation of O_2^- radicals. The
changes in corrosion potential are slow, compared with the rate of radioly-
tic production of radicals, suggesting that oxidation of the UO_2 surface
and not the production rate of radiolytic species is rate-controlling.
Relative rates of oxidation of UO_2 in four different solutions favouring
the formation of selected radicals were investigated [43]. The rates for
this process were much higher for radical species (O_2^-, OH) than for H_2O_2,
which in turn reacted much faster than O_2 [35].

5.2   EFFECT OF DIRECT ALPHA RADIOLYSIS

The strong gamma and beta fields associated with used fuel will decrease by
a factor $>10^3$ in the first few hundred years after disposal. Since the
metallic container is expected to survive this period, groundwater reaching
the fuel after this period will be subjected mainly to alpha radiolysis
[35]. Therefore, it is important to study the impact of alpha radiolysis
of groundwater on UO_2.

We have studied the oxidation of UO_2 fuel by the products of direct alpha
radiolysis of water using alpha sources of various fluxes (5, 50, 250 and
400 μCi[*]) and for different time periods (up to ~50 d) [35,36,38]. We find

---

[*]   1 Ci = 37 GBq

that, at ambient temperatures and in near-neutral solutions (a) the oxida-
tion of UO_2 fuel by the alpha radiolysis of water is a function of the
strength of the alpha flux; (b) an alpha flux greater than or equal to that
from a 250-μCi source (^{241}Am) leads to oxidation beyond the $UO_{2.33}$ (U_3O_7)
stage, which is above the threshold for oxidative dissolution; and (c) an
alpha flux equal to that from a 5-μCi source does not result in UO_2 oxida-
tion beyond the $UO_{2.33}$ stage, and hence may be too weak to force oxidative
dissolution.

As the groundwater reaching the fuel in a geological disposal vault will
probably contain dissolved H_2, resulting from either the corrosion of the
container and fuel sheath or from radiolysis, we have studied the impact
of the presence of H_2 in the groundwater on UO_2 oxidation by the alpha
radiolysis of water. Our studies show that, at room temperature, the
presence of dissolved H_2, at concentrations of $\leq 7 \times 10^{-4}$ mol$\cdot$dm^{-3}, does not
inhibit the oxidation of UO_2. By contrast, at higher temperatures, $\geq 100°C$,
the presence of dissolved H_2 in water reduces the oxidation and dissolution
of UO_2, as a result of the alpha radiolysis of water [44]. This result is
consistent with many observations showing H_2 to be kinetically inert at low
temperatures but more reactive at temperatures $\geq 100°C$.

The expected alpha radiation fields on the used-fuel surface, subsequent
to container failure, are believed to be similar to those obtained with
the 5-μCi source used in our experiments [44]. Thus we conclude that the
alpha radiolysis of water, subsequent to container failure, i.e., after
~500 a, will not lead to fuel oxidation beyond the $UO_{2.33}$ stage. Conse-
quently, we would expect oxidative dissolution at these fluxes to be minor
(Section 4). Hence, the application of a modified solubility-limited model
for UO_2 dissolution [2,75] would appear appropriate in the presence of such
moderate alpha fluxes. Caution should be exercised in using these
conclusions in the direct interpretation of radiolytically induced fuel
dissolution under vault conditions. At low source strengths (~5 μCi), the
geometry of our experimental arrangement will affect the extent of UO_2
oxidation and could lead to an underestimate of the true impact of alpha
radiolysis.

5.3   EFFECT OF GAMMA RADIOLYSIS

The oxidation of UO_2 fuel by the products of gamma radiolysis of water was investigated as a function of radiation-field strength and exposure time. Our studies suggest that the oxidation of UO_2, in irradiated de-oxygenated solutions, consists of two stages [43]. The first stage consists of the growth of a surface film of composition close to $UO_{2.33}$ and similar in thickness to that obtained (over longer exposure periods) in unirradiated oxygenated solutions. The rate of growth of this film appears to be proportional to the square root of the dose rate. The second stage consists of oxidative dissolution of this film (as UO_2^{2+}). This step occurs mainly at higher dose rates. Significant oxidation of UO_2, beyond the $UO_{2.33}$ stage, was observed using radiation fields of ~700 and 7.3 Gy/h (S. Sunder and D.W. Shoesmith, unpublished data). These results suggest that the gamma fields associated with fuels that have been cooled for 10-20 a, currently being used in leaching experiments in several countries, contribute significantly to the UO_2 dissolution rates obtained from these leaching experiments. We have started experiments to determine the longer-term effects of weak gamma fields, associated with used fuel subsequent to container failure, on UO_2 dissolution.

6. IMPACT OF VAULT CHEMISTRY AND SECONDARY PHASE FORMATION

Chemical species dissolved in the groundwater of a vault may affect the kinetics of oxidative dissolution in one of three ways:

   (i)   by direct involvement in the dissolution reaction;

   (ii) by changing the redox conditions that control dissolution; or

   (iii) by forming a transport barrier that inhibits the transport of
         oxidant to, or dissolution product from, the fuel surface.

Complexing anions, such as carbonate, are directly involved in the dissolution reaction, and are discussed in detail in Section 4.2. The kinetics of oxidative dissolution will be significantly affected by chemical processes that cause a change in the vault redox conditions. Such effects, however, cannot be determined simply by measuring or calculating changes of Eh within the vault. The redox conditions at the UO_2 surface are determined by (a) the thermodynamic driving force for dissolution (ΔE_e, equal to the difference in equilibrium potentials for the anodic and cathodic reactions); and (b) the kinetic balance between the oxidative dissolution (an...) and the oxidant reduction (cathodic) reactions [3]. This surface redox condition is specified by a combination of the corrosion potential and the corrosion (dissolution) rate. Consequently, any process within the vault that affects these two parameters will have a direct impact on the kinetics of dissolution.

The impact of such variations under redox conditions could be minimized by a process often termed "redox scavenging." For example, the presence of dissolved lead, a possible matrix material for fuel disposal, inside metal containers can influence the redox potential. Corrosion of lead by oxidants within the vault could render the conditions at the fuel surface less oxidizing [4]. Dissolved Pb^{2+} could also reduce the concentration of aggressive anions in the groundwater, such as carbonate, by precipitation. A similar effect is anticipated with Fe^{2+}, the expected corrosion product from steel containers and present in minerals in the vault. Tests on UO_2 and used fuel in brines [73,76] in the presence of iron showed that the concentrations of uranium, plutonium, technetium, but not cesium, were decreased, because of their reduction by Fe^{2+} to less soluble oxidation states and subsequent precipitation. The presence of Fe^{2+} did not reduce the total release of these elements, suggesting no direct effect on the dissolution kinetics of the fuel. The Fe^{2+} appeared to change the Eh in the near field without affecting the corrosion potential of the fuel.

In contrast to these results, Wuertz and Ellinger [77] claimed that the major decrease (one to two orders of magnitude) in total release of fission products from light-water-reactor (LWR) fuel in salt brines at 200°C when

iron was present could be attributed to the consumption of O_2 by iron corrosion. Also the reduction of radiolytically produced oxidants by iron naturally present in basalt has been invoked to explain why the release of uranium from used fuel was no greater than the release of uranium from simulated used fuel in the presence of basalt [78,79]. Unfortunately, direct studies of the effects of redox modifiers on UO_2 dissolution kine-- tics are difficult and, so far, inconclusive.

The formation of secondary phases in contact with the UO_2 surface may have an accelerating or inhibiting effect on dissolution, depending on the nature of the dissolution process. If the reaction is close to equili- brium, i.e., the surface concentration of dissolved uranium is close to the solubility of the phase on the UO_2 surface, then formation of a secondary phase, at a finite distance from the fuel surface, could act as a "thermo- dynamic pump" and lead to an increase in the dissolution rate. At present, there is no experimental evidence for such a process, though the calcula- tions of Garisto and Garisto [80] show that such an effect could be impor- tant at long times (10^3 to 10^4 a). A more likely scenario is that the formation of secondary phases on the UO_2 surface will inhibit dissolution by providing a semi-impermeable layer for oxidant transport to, or dis- solved uranium transport away from, the UO_2 surface. According to Wang and Katayama [81], secondary phase formation is enhanced at higher temperatures (150°C) as a result of accelerated dissolution and a negative temperature coefficient of solubility. They claim that precipitation on the dissolving surface inhibits dissolution.

The formation of secondary phases, such as coffinite ($U(SiO_4)_{1-x} (OH)_{4x}$) and weeksite and/or boltwoodite (hydrated potassium-uranium-silicate phases), has been observed in high-temperature (300°C) used-fuel tests in the presence of basalt rock [76]. Since reducing conditions are produced in the presence of basalt, the production of secondary phases containing U^{4+} is not surprising. Little was said, however, about the impact of their presence on dissolution rates. More recently, the formation of secondary phases containing U^{6+} has been observed at lower temperatures, 85 to 90°C, in dissolution experiments carried out using oxidizing groundwaters

[82-84]. These authors reported a decrease in uranium dissolution rates with the buildup of the secondary phases on the UO_2 surface.

The results of experiments on CANDU fuel [46] showed that dissolution rates decreased as a function of temperature in granitic groundwaters, but increased in distilled water. This was attributed to the formation of passivating uranyl phases, such as $NaUO_3$ and $Na_2U_2O_7$; however, it is more likely to be due to the formation of mineralized films [82-84].

7. PHYSICAL FACTORS

In addition to the chemical factors discussed above, various physical characteristics of the fuel, e.g., crystallinity, grain size, surface area, solid-state defects, etc., will also affect its dissolution rate [4]. Although UO_2 fuel has been characterized extensively [85,86], little is known that correlates the various physical factors to the dissolution rate.

The measurement of dissolution rates by Nel [87] and electrochemical studies by Nicol and Needes [88] showed that the dissolution rate decreases with a decrease in the number of defects in the UO_2 structure. Nicol and Needes studied five different samples, ranging from single crystals ($UO_{2.03}$) to sintered pellets ($UO_{2.01}$) and fused polycrystalline material ($UO_{2.10}$ to $UO_{2.14}$) and reported that the sintered pellets were 20 to 50 times more reactive than the single crystal. They attributed the low reactivity of the single crystal to the absence of grain boundaries and pores (defects). The increased reactivity of the sintered pellets was attributed to the small size of crystallites, leading to a high surface density of grain boundaries, i.e., higher surface area and greater number of reactive sites. No direct correlation with purity (as measured by the oxygen:uranium ratio) was observed. The electrochemical tests of Johnson et al. showed extensive grain-boundary etching, indicating higher reactivity at the edges [30], i.e., areas known to contain a greater number of defects and reactive sites.

In general, an increase in the number of defects or a decrease in particle size will lead to an increase in the number of active sites at the fuel surface, which will enhance its dissolution rate. Thermal cycling, nuclear fission and radiation damage during reactor operation tend to increase the number of defects in UO_2 fuel [89]. Although the dissolution rates of the fuel will depend upon its history in the reactor, the general chemical mechanism of its dissolution is not expected to change [4].

More recently, differences in the reactivity of UO_2 have been correlated with the semiconducting properties of the solid [74]. As discussed in Section 4.1, both the mechanism and the kinetics of the cathodic reactions that drive oxidative dissolution change with surface composition and conduction type (p- or n-type). Preliminary results suggest that these factors also affect the anodic dissolution reaction.

8. APPROACHES TO MODELLING UO_2 DISSOLUTION

Predicting the release rates of radionuclides from fuel will be easier than predicting their release from the vault. This is due to the complexity of the near-field chemistry and its modification by processes such as container corrosion. Any model successfully predicting release from the vault will involve the specification of the transport regime for dissolved radionuclides within the vault, and how it is modified by adsorption, precipitation/redissolution, and other reactions [75,80,90].

In these models, the UO_2 dissolution rate represents the input boundary conditions for the transport model at the fuel/vault interface. Generally, dissolution is assumed to be controlled either by the solubility of the phase present on the UO_2 surface [2,91] or by a constant irreversible rate [75,77]. The use of a solubility-limited boundary condition defines the dissolution process as being chemical, as opposed to electrochemical, in nature and is justified under reducing conditions [2,75]. Under oxidizing conditions such a boundary condition is no longer justified, since dissolution is irreversibly driven by oxidants present in the vault. The redox

condition at the fuel surface, expressed as the corrosion potential, is established by the balance between the kinetics of the anodic (UO_2 dissolution) and cathodic (oxidant reduction) reactions [4]. The achievement of a solubility-limited input boundary condition is unlikely.

Attempts have been made to specify the redox conditions for which the solubility-limited and kinetic oxidative models are applicable [3,4,40]. Figure 6 summarizes the surface chemistry of UO_2 as a function of surface redox conditions (corrosion potential) at pH ~ 9.5, a likely value in granitic groundwaters. Located on this scale are the corrosion potentials measured in oxygen-saturated and nitrogen-degassed solutions. The latter measurements represent the least oxidizing conditions experimentally achievable at 25°C ($[O_2]$ ~ 10^{-9} mol·L^{-1}) without the addition of reducing agents. Our XPS results show that, even under these conditions, slight oxidation of UO_2 is obtained. The two hatched regions show the redox conditions where the two models can be reasonably assumed to apply.

The redox condition above which the solubility-limited model no longer applies is not well defined. If we accept that a surface composition close to $UO_{2.33}$ is required for oxidative dissolution, our XPS and electrochemical results suggest that a transition between the two models will occur around -100 mV (vs. SCE) (S. Sunder and D.W. Shoesmith, unpublished data).

The use of a constant rate to describe oxidative dissolution, equivalent to a constant-concentration source boundary condition for the transport model, neglects the basic electrochemical nature of the dissolution process and how it is affected by vault parameters. This review has discussed these parameters in some detail. Using an electrochemical approach, the anodic dissolution rate of fuel can be expressed by equations of the type

$$I_A = k_{UO_2}[X]^m[Y]^p f(E) \tag{10}$$

where k_{UO_2} is a heterogenerous rate constant, and the rate is dependent on the concentration of species X and Y (probably HCO_3^- and H^+) with reaction orders m and p respectively. The term $f(E)$ expresses the dependence of the

REDOX CHEMISTRY OF UO_2

pH ~ 9.5
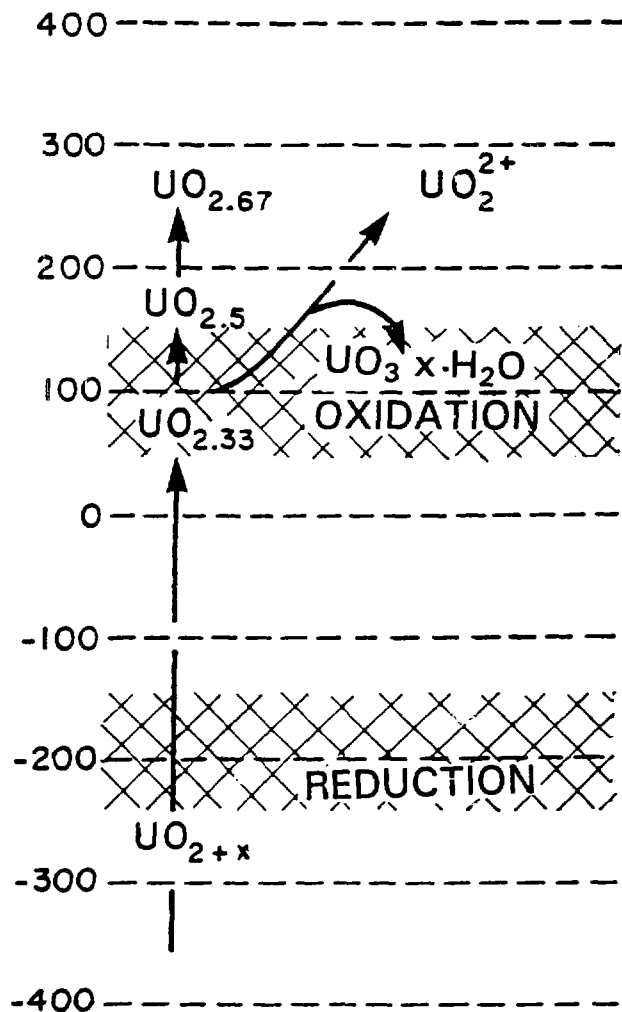
FIGURE 6: Surface Chemistry of UO_2 Oxidation/Dissolution as a Function of Surface Redox Conditions

dissolution rate on redox conditions expressed electrochemically. A similar expression can be written relating the cathodic current to the potential:

$$I_c = k_{ox}[Ox]^q f'(E) \tag{11}$$

where k_{ox} represents the rate constant of the oxidant Ox causing UO_2 oxidation and being reduced in the process with a reaction order q.

If more than one cathodic reaction occurs, the total cathodic current will be the sum of the individual currents [3]. The equations for anodic and cathodic currents can be related through the corrosion potential and an expression for the dissolution rate derived. The basis for this model and its extension to include variations in fuel reactivity have been published [40]. The mathematical details and experimental justification remain to be developed.

In order to formulate such a model, it is necessary to specify the form of Equation (11). In radiolytically decomposed water, dissolution will be driven by a number of oxidants, such as $OH^{\cdot}$, O_2^-, H_2O_2 and O_2, which react at very different rates. To model the full kinetic impact of radiolysis, a model is required that distinguishes between the rate of reaction of each species with UO_2. Such a model has been proposed by Christensen and Bjergbakke [92,93]. The model is based on a reaction mechanism in which the dissolution is initiated by reactions with H_2O_2, OH and O_2^- radicals. This model assumes that a monomolecular surface layer of UO_2 is dissolved within the range of alpha particles (~ 30 μm in water) or, for gamma radiation, within the diffusion range of the radicals formed during the radiolysis. This assumption was necessary to use the formalism (computer programs) devised to study the reaction kinetics in a homogeneous medium. In the absence of kinetic data for uranium oxides, reaction rates from the literature for other oxides were used. Our experiments on the effects of specific radicals are designed to provide the data needed to improve this model [42,43].

Also, by studying the effect of dose rate on corrosion potential and surface composition, we hope to relate the corrosion rate of UO_2 to the concentration of specific radiolysis products. Such a relationship will enable us to predict the impact of specific radiation dose rates, and hence to assess the vulnerability of fuel to radiolytically induced dissolution under vault conditions.

The impact of secondary phase formation on the kinetics of the oxidative dissolution of UO_2 is probably the most complex and least understood aspect of the process [94]. Since dissolution is irreversible, the rate will not be accelerated by the thermodynamic-pump effect described by Garisto and Garisto [80] for the solubility-limited model. Consequently, the rate predicted under oxidizing conditions using the above approach will be the maximum dissolution rate under specific conditions. The true rate may be reduced by slow transport processes within the buffer or through low-permeability secondary phases on the surface of the fuel.

ACKNOWLEDGEMENTS

REFERENCES

1. Parks, G.A. and D.C. Pohl. 1988. Hydrothermal solubility of uraninite. Geochim. Cosmochim. Acta 52, 863-875.

2. Garisto, N.C. and D.M. Leneveu. 1988. A vault model for the assessment of used fuel disposal in Canada. Materials Research Society Symposia Proceedings 112 (Scientific Basis for Nuclear Waste Management XI), 313-322.

3. Shoesmith, D.W., S. Sunder, B.M. Ikeda and F. King. 1989. The development of a mechanistic basis for modelling fuel dissolution and container failure under waste vault conditions. Materials Research Society Symposia Proceedings 127 (Scientific Basis for Nuclear Waste Management XII), 279-291. Also Atomic Energy of Canada Limited Reprint, AECL-9827.

4. Johnson, L.H. and D.W. Shoesmith. 1988. Spent fuel. In Radio-active Waste Forms for the Future (W. Lutze and R.C. Ewing, editors). Elsevier Science Publishers B.V., 635-698. Also Atomic Energy of Canada Limited Reprint, AECL-9583.

5. Smith, D.K., B.E. Scheetz, C.A.F. Anderson and K.L. Smith. 1982. Phase relations in the uranium-oxygen-water system and its signi-ficance on the solubility of nuclear waste forms. Uranium 1, 79-111.

6. Gronvold, F. 1955. High-temperature X-ray study of uranium oxides in the UO_2-U_3O_8 region. J. Inorg. Nucl. Chem. 1, 357-370.

7. Willis, B.T.M. 1978. The defect structure of hyper-stoichiometric uranium dioxide. Acta Crystallogr. Sect. A34, 88-90.

8. Bevan, D.J.M., I.E. Grey and B.T.M. Willis. 1986. The crystal structure of β-U_4O_{9-y}. J. Solid State Chem. 61, 1-7.

9.   Willis, B.T.M. 1987. Crystallographic study of anion-excess uranium oxides. J. Chem. Soc. Faraday Trans. 2 $\underline{83}$, 1073-1081.

10. Willardson, R.K., J.W. Moody and H.L. Goering. 1958. The electrical properties of uranium oxides. J. Inorg. Nucl. Chem. $\underline{6}$, 19-33.

11. Aronson, S., J.E. Rulli and B.E. Schaner. 1961. Electrical properties of nonstoichiometric uranium dioxide. J. Chem. Phys. $\underline{35}$, 1382-1388.

12. Dudney, N.J., R.L. Coble and H.L. Tuller. 1981. Electrical conductivity of pure and yttria-doped uranium dioxide. J. Am. Ceram. Soc. $\underline{64}$, 627-631.

13. Catlow, C.R.A. 1977. Point defect and electronic properties of uranium dioxide. Proc. R. Soc. London Ser. $\underline{A353}$, 533-561.

14. Schoenes, J. 1980. Electronic transitions, crystal field effects and phonons in UO_2. Phys. Rep. $\underline{63}$, 301-336.

15. Manes, L. and J. Naegele. 1976. On the electronic properties of actinide oxides. $\underline{In}$ Plutonium and Other Actinides (H. Blank and R. Linder, editors). North-Holland, Amsterdam, Netherlands, 361-382.

16. Hoekstra, H.R., A. Santoro and S. Siegel. 1961. The low temperature oxidation of UO_2 and U_4O_9. J. Inorg. Nucl. Chem. $\underline{18}$, 166-178.

17. Hoekstra, H.R., S. Siegel and F.X. Gallagher. 1970. The uranium-oxygen system at high pressure. J. Inorg. Nucl. Chem. $\underline{32}$, 3237-3248.

18. Aléonard, S., Y. Le Fur, J.C. Champarnaud-Mesjard, B. Frit and M. Th. Roux. 1983. Relations structurales entre U_3O_8 et quelques fluorures mixtes de formules $M_2M_3'F_{11}$, $MM_2'F_7$ et $MM_3'F_{10}$. J. Solid State Chem. $\underline{46}$, 87-100.

19.   Dharwadkar, S.R., M.S. Chandrasekharaiah and M.D. Karkhanavala,
      1978. A physicochemical study of the uranium-oxygen system between
      $UO_{2.65}$ and $UO_{2.67}$. J. Nucl. Mater. 71, 268-276.

20.   O'Hare, P.A.G., B.M. Lewis and S.N. Nguyen. 1988. Thermochemistry
      of uranium compounds. XVII. Standard molar enthalpy of formation
      at 298.15 K of dehydrated schoepite $UO_3 \cdot 0.9H_2O$. Thermodynamics of
      (schoepite + dehydrated schoepite + water). J. Chem. Thermodyn. 20,
      1287-1296.

21.   Hoekstra, H.R., and S. Siegel. 1973. The uranium trioxide-water
      system. J. Inorg. Nucl. Chem. 35, 761-779.

22.   Keim, R. 1978. Uran. Gmelin Handbuch der Anorganischen Chemie.
      Volume C2. Springer-Verlag, Heidelberg, Germany.

23.   Bruno, J., I. Casas and I. Puigdomenech. 1988. The kinetics of
      dissolution of $UO_2(s)$ under reducing conditions. Radiochim. Acta
      44/45, 11-16.

24.   Nicol, M.J., C.R.S. Needes and N.P. Finkelstein. 1975. Electro-
      chemical model for the leaching of uranium dioxide. 1. Acid media.
      In Leaching and Reduction in Hydrometallurgy (A.R. Burkin, editor).
      Inst. Min. Metall., London, UK, 1-11.

25.   Needes, C.R.S., M.J. Nicol and N.P. Finkelstein. 1975. Electro-
      chemical model for the leaching of uranium dioxide. 2. Alkaline
      carbonate media. In Leaching and Reduction in Hydrometallurgy (A.R.
      Burkin, editor). Inst. Min. Metall., London, UK, 12-19.

26.   Bard, A.J. and L.R. Faulkner. 1980. Electrochemical Methods.
      Fundamentals and Applications. John Wiley and Sons, New York, NY.

27.   Sunder, S., D.W. Shoesmith, M.G. Bailey, F.W. Stanchell and
       N.S. McIntyre. 1981. Anodic oxidation of UO_2. Part I. Electro-
       chemical and X-ray photoelectron spectroscopic studies in neutral
       solutions. J. Electroanal. Chem. 130, 163-179. Also Atomic Energy
       of Canada Limited Reprint, AECL-7139.

28.   McIntyre, N.S., S. Sunder, D.W. Shoesmith and F.W. Stanchell. 1981.
       Chemical information from XPS - applications to the analysis of
       electrode surfaces. J. Vac. Sci. Technol. 18, 714-721. Also Atomic
       Energy of Canada Limited Reprint, AECL-7002.

29.   Sunder, S., D.W. Shoesmith, M.G. Bailey and G.J. Wallace. 1982.
       Mechanism of oxidative dissolution of UO_2 under waste disposal vault
       conditions. In Canadian Nuclear Society International Conference on
       Radioactive Waste Management, Conference Proceedings, Winnipeg, MB,
       1982, 398-405.

30.   Johnson, L.H., D.W. Shoesmith, G.E. Lunansky, M.G. Bailey and
       P.R. Tremaine. 1982. Mechanisms of leaching and dissolution of UO_2
       fuel. Nucl. Technol. 56, 238-253. Also Atomic Energy of Canada
       Limited Reprint, AECL-6992.

31.   Sunder, S., D.W. Shoesmith, M.G. Bailey and G.J. Wallace. 1983.
       Anodic oxidation of UO_2. Part II. Electrochemical and X-ray photo-
       electron spectroscopic studies in alkaline solutions. J. Electro-
       anal. Chem. 150, 217-228. Also Atomic Energy of Canada Limited
       Reprint, AECL-7852.

32.   Shoesmith, D.W., S. Sunder, M.G. Bailey and D.G. Owen. 1983.
       Anodic oxidation of UO_2. Part III. Electrochemical studies in
       carbonate solutions. In Passivity of Metals and Semiconductors,
       Proceedings of the 5th International Symposium on Passivity,
       Bombannes, France, 1983, 125-130. Also Atomic Energy of Canada
       Limited Reprint, AECL-7956.

33.   Shoesmith, D.W., S. Sunder, M.G. Bailey, G.J. Wallace and
      F.W. Stanchell. 1984. Anodic oxidation of UO_2. Part IV. X-ray
      photoelectron spectroscopic and electrochemical studies of film
      growth in carbonate-containing solutions. Appl. Surf. Sci. 20,
      39-57. Also Atomic Energy of Canada Limited Reprint, AECL-8174.

34.   Bailey, M.G., L.H. Johnson and D.W. Shoesmith. 1985. The effects
      of the alpha-radiolysis of water on the corrosion of UO_2. Corros.
      Sci. 25, 233-238. Also Atomic Energy of Canada Limited Reprint,
      AECL-8430.

35.   Shoesmith, D.W., S. Sunder, L.H. Johnson and M.G. Bailey. 1985.
      Oxidation of CANDU UO_2 fuel by the alpha-radiolysis products of
      water. Materials Research Society Symposia Proceedings 50 (Scienti-
      fic Basis for Nuclear Waste Management IX), 309-316. Also Atomic
      Energy of Canada Limited Reprint, AECL-8888.

36.   Sunder, S., D.W. Shoesmith, L.H. Johnson, M.G. Bailey and
      G.J. Wallace. 1986. Effect of alpha radiolysis of water on CANDU[TM]
      fuel oxidation. In Canadian Nuclear Society 2nd International
      Conference on Radioactive Waste Management, Conference Proceedings,
      Winnipeg, MB, 1986, 625-631.

37.   Shoesmith, D.W., S. Sunder, M.G. Bailey, and G.J. Wallace. 1986.
      Mechanism of oxidation and dissolution of CANDU fuel. In Canadian
      Nuclear Society 2nd International Conference on Radioactive Waste
      Management, Conference Proceedings, Winnipeg, MB, 1986, 674-679.

38.   Sunder, S., D.W. Shoesmith, L.H. Johnson, G.J. Wallace, M.G. Bailey,
      and A.P. Snaglewski. 1987. Oxidation of CANDU[TM] fuel by the
      products of the alpha radiolysis of groundwater, Materials Research
      Society Symposia Proceedings 84 (Scientific Basis for Nuclear Waste
      Management X), 102-113. Also Atomic Energy of Canada Limited
      Reprint, AECL-9296.

39.   Shoesmith, D.W., S. Sunder, M.G. Bailey, and G.J. Wallace. 1988.
        Anodic oxidation of UO_2. V. Electrochemical and X-ray photoelec-
        tron spectroscopic studies of film-growth and dissolution in
        phosphate-containing solutions, Can. J. Chem. 66, 259-265.

40.   Johnson, L.H., D.W. Shoesmith and S. Stroes-Gascoyne. 1988. Spent
        fuel: characterization studies and dissolution behaviour under
        disposal conditions. Materials Research Society Symposia Proceed-
        ings 112 (Scientific Basis for Nuclear Waste Management XI), 99-113.
        Also Atomic Energy of Canada Limited Reprint, AECL-9651.

41.   Shoesmith, D.W., S. Sunder, M.G. Bailey, and G.J. Wallace. 1989.
        The corrosion of nuclear fuel (UO_2) in oxygenated solutions.
        Corros. Sci. 29, 1115-1128.

42.   Sunder, S. D.W. Shoesmith, H. Christensen, M.G. Bailey and N.
        Miller. 1989. Electrochemical and X-ray photoelectron spectroscopic
        studies of UO_2 fuel oxidation by specific radicals formed during
        radiolysis of groundwater. Materials Research Society Symposia
        Proceedings 127 (Scientific Basis for Nuclear Waste Management XII),
        317-324. Also Atomic Energy of Canada Limited Reprint, AECL-9597.

43.   Sunder, S., D.W. Shoesmith, H. Christensen, N.H. Miller and
        M.G. Bailey. 1990. Oxidation of UO_2 fuel by radicals formed during
        radiolysis of water. Materials Research Society Symposia Proceed-
        ings 176 (Scientific Basis for Nuclear Waste Management XIII),
        457-464. Also Atomic Energy of Canada Limited Reprint, AECL-10093.

44.   Sunder, S., G.D. Boyer and N.H. Miller. 1990. XPS studies of UO_2
        oxidation by alpha radiolysis of water at 100°C. J. Nucl. Mater.
        175, 163-169. Also Atomic Energy of Canada Limited Reprint,
        AECL-10303.

45.   Sunder, S., D.W. Shoesmith, R.J. Lemire, M.G. Bailey and
        G.J. Wallace. 1991. The effect of pH on the corrosion of nuclear
        fuel (UO_2) in oxygenated solutions. Corros. Sci. 32, 373-386. Also
        Atomic Energy of Canada Limited Reprint, AECL-10093.

46.   Thomas, G.F. and G. Till. 1984. The dissolution of unirradiated
        UO_2 fuel pellets under simulated disposal conditions. Nucl. Chem.
        Waste Manage. 5, 141-147.

47.   Gascoyne, M. 1988. Reference groundwater composition for a depth
        of 500 m in the Whiteshell Research Area - comparison with synthetic
        groundwater WN-1. Atomic Energy of Canada Limited Technical Record,
        TR-463.

48.   Lemire, R.J. 1988. Effects of high ionic strength groundwaters on
        calculated equilibrium concentrations in the uranium-water system.
        Atomic Energy of Canada Limited Report, AECL-9549.

49.   Lemire, R.J. and F. Garisto. 1989. The solubility of U, Nb, Pu, Th
        and Tc in a geological disposal vault for used nuclear fuel. Atomic
        Energy of Canada Limited Report, AECL-10009.

50.   Grenthe, I., D. Ferri, F. Salvatore and G. Riccio. 1984. Studies
        on metal carbonate equilibria. Part 10. A solubility study of the
        complex formation in the uranium (VI)-water-carbon dioxide (g)
        system at 25°C. J. Chem. Soc. Dalton Trans. 11, 2439-2443.

51.   Lemire, R.J. and P.R. Tremaine. 1980. Uranium and plutonium
        equilibria in aqueous solutions to 200°C. J. Chem. Eng. Data. 25,
        361-370. Also Atomic Energy of Canada Limited Reprint, AECL-6655.

52.   Paquette, J. and R.L. Lemire. 1981. A description of the chemistry
        of aqueous solutions of uranium and plutonium to 200°C using
        potential-pH diagrams. Nucl. Sci. Eng. 79, 26-48. Also Atomic
        Energy of Canada Limited Reprint, AECL-7037.

53.   Langmuir, D. 1978. Uranium solution-mineral equilibria at low
        temperatures with applications to sedimentary ore deposits.
        Geochim. Cosmochim. Acta 42, 547-569.

54.   Wilson, C.N. 1988. Summary of results from the Series 2 and Series 3 NNWSI bare fuel dissolution tests. Materials Research Society Symposia Proceedings 127 (Scientific Basis for Nuclear Waste Management XI), 473-483.

55.   Allard, B., S.A. Larsson, A.L. Tullborg, P. Wikberg. 1983. Chemistry of deep groundwaters from granitic bedrock. Swedish Nuclear Fuel Supply Co./Division KBS Report, KBS-TR-83-59.

56.   Li. W.C., D.M. Victor, L.C. Chakrabarti. 1980. Effect of pH and uranium concentration on interaction of uranium(VI) and uranium(IV) with organic ligands in aqueous solutions. Anal. Chem. 52, 520-523.

57.   Choppin, G.R. 1988. Humics and radionuclide migration. Radiochim. Acta 44/45, 23-28.

58.   Christensen, H. 1978. γ-radiolysis of organic compounds and α-radiclysis of water. Studsvik Technical Report E2-78/15, Studsvik Energiteknik AB, Nykoping, Sweden.

59.   Eriksen, T.E. and A. Jacobsson. 1981. Diffusion of hydrogen, hydrogen sulfide and large molecular weight anions in bentonite. Swedish Nuclear Fuel Supply Co./Division KBS Report, KBS-TR-82-17.

60.   Stone, A.T. and J.J. Morgan. 1987. Reductive dissolution of metal oxides. In Aquatic Surface Chemistry (W. Stumm, editor). J. Wiley, New York, NY, 221-254.

61.   Allen, A.O. 1961. The Radiation Chemistry of Water and Aqueous Solutions. D. Van Nostrand Co. Inc., Princeton, NJ.

62.   Laxen, P.A. 1971. The dissolution of UO_2 as an electron transfer reaction. IAEA Report No. IAEA-SM-135/29, 321-330.

63.   Scott, P.D., D. Glasser and M.J. Nicol. 1977. Kinetics of dissolu-
        tion of β-uranium trioxide in acid and carbonate solutions. J.
        Chem. Soc. Dalton Trans., 1939-1946.

64.   Kanevskii, E.A., G.M. Nesmeyanova, L.N. Kuz'mina and G.A. Dymkova.
        1975. Kinetics of the oxidation of powdered uranium dioxide in a
        sulfuric acid solution by vanadium(v). I. Empirical equation for
        the speed of the reaction process and area in which it takes place.
        Radiokhimiya 17(1), 110-115.

65.   Nicol, M.J. and C.R.S. Needes. 1972. A potentiostatic study of the
        anodic dissolution of uranium dioxide in aqueous solutions. Natl.
        Inst. Metall., Repub. S. Afr. Report No. 1448.

66.   Du Preez, J.G.H., D.C. Morris and C.P.J. Van Vuuren. 1981. The
        chemistry of uranium. XXVII. Kinetics of the dissolution of
        uranium dioxide powder in a solution containing radium carbonate,
        sodium bicarbonate, and potassium cyanide. Hydrometallurgy 6,
        197-201.

67.   Forward, F.A. and J. Halpern. 1953. Carbonate leaching of uranium
        ores I. Description of the pressure-leach process and its applica-
        tion to pitchblende ores. Trans. Can. Inst. Mining Met. 56,
        354-360.

68.   Hiskey, J.B. 1979. Kinetics of uranium dioxide dissolution in
        ammonium carbonate. Trans. Inst. Min. Metall., Sect. C, 88,
        C145-C152.

69.   Schortmann, W.E. and M.A. DeSesa. 1958. Kinetics of the dissolu-
        tion of uranium dioxide in carbonate-bicarbonate solutions. In 2nd
        UN International Conference on the Peaceful Uses of Atomic Energy,
        Conference Proceedings, Geneva, Switzerland, 1958, 3, 333-341.

70.   Grandstaff, D.E. 1976. A kinetic study of the dissolution of
        uraninite. Econ. Geol., Bull. Soc. Econ. Geol. 71, 1493-1506.

71. Eary, L.E. and L.M. Cathles. 1983. A kinetic model of uranium
     dioxide dissolution in acid, hydrogen peroxide solutions that
     includes uranium peroxide hydrate precipitation. Metall. Trans. B
     14B, 325-334.

72. Johnson, L.H. and H.H. Joling. 1982. The dissolution of irradiated
     fuel under hydrothermal conditions. Materials Research Society
     Symposia Proceedings 6 (Scientific Basis for Nuclear Waste
     Management IV), 321-327.

73. Gray, W.J. and G.L. McVay. 1984. Comparison of spent fuel and UO_2
     release in salt brines. In Proceedings of the 3rd Spent Fuel Work-
     shop, Stockholm, Sweden, 1984, Swedish Nuclear Fuel Supply
     Co./Division KBS Report, KBS-83-76.

74. Hocking, W.H., J.S. Betteridge and D.W. Shoesmith. 1991. The
     mechanism of oxygen reduction on UO_2. Atomic Energy of Canada
     Limited Report, AECL-10402.

75. Garisto, N.C. and F. Garisto. 1986. The dissolution of UO_2: a
     thermodynamic approach. Nucl. Chem. Waste Manage. 6, 203-211. Also
     Atomic Energy of Canada Limited Reprint, AECL-8887.

76. Barner, J.O., W.J. Gray, G.L. McVay and J.W. Schade. 1986. Inter-
     active leach tests of UO_2 and spent fuel with waste package compo-
     nents in salt brine. Pacific Northwest Laboratory Report,
     PNL-4898-SRP.

77. Wuertz, R. and M. Ellinger. 1985. Source term for the activity
     release from a repository for spent LWR fuel. Materials Research
     Society Proceedings 50 (Scientific Basis for Nuclear Waste
     Management IX), 393-400.

78.   Myers, J., M.J. Apted and J.J. Mazer. Hydrothermal reaction of
       simulated waste forms with basalt under conditions expected in a
       nuclear waste repository in basalt. Rockwell Hanford Operations
       Report, RHO-BW-ST-59-P.

79.   Schramke, J.A., S.A. Simonson and D.G. Coles. 1984. A report on
       the status of hydrothermal testing of fully radioactive waste forms
       and basalt repository waste package components. Rockwell Hanford
       Operations Report, SD-BWI-TI-253.

80.   Garisto, F. and N.C. Garisto. 1986. The effect of precipitation on
       radionuclide release from used fuel. In Canadian Nuclear Society
       2nd International Conference on Radioactive Waste Management,
       Conference Proceedings, Winnipeg, MB, 1986, 645-648.

81.   Wang, R. and Y.B. Katayama. 1982. Dissolution mechanism for UO_2
       and spent fuel. Nucl. Chem. Waste Manage. 3, 83-90.

82.   Lahalle, M.P., J.C. Krupa, R. Guillaumont, M. Genet, G.C. Allen, and
       N. Holmes. 1988. Surface analysis of uranium dioxide leached in
       mineral water studied by X-ray photoelectron spectroscopy. Mater-
       ials Research Society Symposia Proceedings 127 (Scientific Basis for
       Nuclear Waste Management XII), 351-356.

83.   Wilson, C.N. and W.J. Gray. 1990. Measurement of soluble nuclide
       dissolution rates from spent fuel. Materials Research Society
       Symposia Proceedings 176 (Scientific Basis for Nuclear Waste
       Management XIII), 489-498.

84.   Bates, J.K., B.S. Tani, E. Veleckis and D.J. Wronkiewicz. 1990.
       Identification of secondary phases formed during unsaturated reac-
       tion of uranium dioxide with water. Materials Research Society
       Symposia Proceedings 176 (Scientific Basis for Nuclear Waste
       Management XIII), 499-506.

85.   See articles in J. Chem. Soc., Faraday Trans. 2 83, 1065-1285 (1987).

86.   Reimus, P.W. and S.A. Simonson. 1988. Radionuclide release from
       spent fuel under geologic disposal conditions: an overview of
       experimental and theoretical work through 1985. Pacific Northwest
       Laboratories Report, PNL-5551, B.1-B.14.

87.   Nel, H.J. 1958. Discussion of the attrition of uraninite. Geol.
       Soc. S. Afr. Trans. 61, 194.

88.   Nicol, M.J., and C.R.S. Needes. 1975. The anodic dissolution of
       uranium dioxide - I. In perchlorate solutions. Electrochim. Acta
       20, 585-589.

89.   Matzke, H. 1987. Atomic transport properties in UO_2 and mixed
       oxides $(U,Pu)O_2$. J. Chem. Soc., Faraday Trans. 2 83, 1121-1142.

90.   Haworth, A., S.M. Sharland, P.W. Tasker and C.J. Tweed. 1988.
       Evolution of the groundwater chemistry around a nuclear waste
       repository. Materials Research Society Symposia Proceedings 112
       (Scientific Basis for Waste Management XI), 425-434.

91.   Goodwin B.W., R.J. Lemire and L.H. Johnson. 1982. A stochastic
       model for the dissolution of irradiated UO_2 fuel. Canadian Nuclear
       Society International Conference on Radioactive Waste Management,
       Conference Proceedings, Winnipeg, MB, 1982, 298-304.

92.   Christensen, H. and E. Bjergbakke. 1986. Application of CHEMSIMUL
       for groundwater radiolysis. Nucl. Chem. Waste Manage. 6, 265-270.

93.   Christensen, H. and E. Bjergbakke. 1986. Radiation induced
       dissolution of uranium dioxide. Materials Research Society Symposia
       Proceedings 84 (Scientific Basis for Nuclear Waste Management X),
       115-122.